

TABLE II. Parameters for gold contacts on three semiconductors. Values of  $\chi$  are from Table I. Values of  $\phi_{Au}$  were determined *in situ* by measurements of contact potential, while  $\Delta\phi_{ms}$  results were derived from capacitance measurements.

Material	$\chi$ (eV)	$\phi_{Au}$ (eV)	$\chi - \phi_{Au}$ (eV)	$\Delta\phi_{ms}$ (eV)
CdS	4.79	5.59	0.80	0.79
CdTe	4.28	5.08	0.80	0.63
ZnO	4.57	5.59	1.02	0.90

Table II. Fair agreement with Eq. (1) is obtained, provided the appropriate metal work function is used. One does not expect exact agreement with Eq. (1) since it does not take into account modifications in the surface double layers when the two materials are placed in intimate contact.

## ACKNOWLEDGMENTS

The author wishes to acknowledge important contributions to this work by a number of his colleagues. M. Aven provided samples of ZnSe and ZnTe, made a number of special firings for purification of these and other crystals, and provided valuable consultation in many aspects of the work. R. E. Halsted and H. D. Coghill supplied crystals of CdTe. P. D. Johnson made his vacuum spectrometer available for the photoelectric measurements. D. T. F. Marple provided unpublished measurements of reflectivity of CdTe. The applicability of surface photovoltage measurements to this work arose out of conversations with D. A. Cusano. Technical assistance throughout this program has been provided by J. Z. Devine.

## Many-Body Effects in the Optical Properties of Semiconductors\*

A. BARDASIS

*Department of Physics and Astronomy, University of Maryland, College Park, Maryland*

AND

DANIEL HONE

*Department of Physics and Laboratory for Research on the Structure of Matter,  
University of Pennsylvania, Philadelphia, Pennsylvania*

(Received 2 August 1966)

The high-frequency optical absorption of semiconductors of the diamond structure type has been investigated theoretically for the almost-free-electron energy-band model isotropically extended to three dimensions. Model-independent arguments show that ignoring interactions between particles so that all excitations are infinitely long-lived leads to calculated values of the absorptive part of the dielectric constant,  $\epsilon_2(q \rightarrow 0, \omega)$ , well below the experimental results for Ge and Si. Within our model, we have investigated self-energy and vertex corrections to  $\epsilon_2(\omega)$  due to many-body effects resulting from the Coulomb interactions between particles. Both these corrections significantly raise the theoretical value of  $\epsilon_2(\omega)$ , bringing them substantially closer to experimental ones.

### I. INTRODUCTION

THE subject of the optical properties of both metals and semiconductors<sup>1</sup> is usually investigated experimentally through the determination of the reflectance and characteristic energy-loss functions, which are directly interpretable in terms of the complex dielectric constant

$$\epsilon(\mathbf{q}, \omega) = \epsilon_1(\mathbf{q}, \omega) + i\epsilon_2(\mathbf{q}, \omega) \quad (1.1)$$

in the optical ( $\mathbf{q} \rightarrow 0$ ) limit.

Ehrenreich and Philipp have considered theoretical analyses of their experimental results for the metals Ag and Cu,<sup>2</sup> and semiconductors of the diamond structure type, such as Si and Ge.<sup>3</sup> In this paper we are interested

in the latter set of experiments. Specifically, we concern ourselves with the absorptive part of the dielectric constant.

One of the main difficulties with a theoretical development for  $\epsilon_2(\omega)$  in the semiconductor case is that some model for the electronic band structure must be considered, since an external photon of energy  $\hbar c q$  cannot create an electron-hole pair in a free electron gas in the  $q \rightarrow 0$  limit without violating energy-momentum conservation. Therefore,  $\epsilon_2(\omega)$  would vanish in the absence of a lattice, as it does in the usual random-phase approximation (RPA)<sup>4</sup> treatment of the free-electron gas. Once crystal structure is introduced, however, momentum need be conserved only up to a reciprocal lattice vector, so that interband transitions give rise to a finite value for  $\epsilon_2(\omega)$ , for  $\omega$ 's larger than the minimum inter-

\* Supported in part by the Advanced Research Projects Agency.

<sup>1</sup> J. Tauc, in *Progress in Semiconductors*, edited by A. F. Gibson and R. E. Burgess (Temple Press Books, Ltd., London, 1965), Vol. IX.

<sup>2</sup> H. Ehrenreich and H. R. Philipp, *Phys. Rev.* **128**, 1622 (1962).

<sup>3</sup> H. R. Philipp and H. Ehrenreich, *Phys. Rev.* **129**, 1550 (1963).

<sup>4</sup> David Pines, *Elementary Excitations in Solids* (W. A. Benjamin and Company, Inc., New York, 1964), Chap. 3.

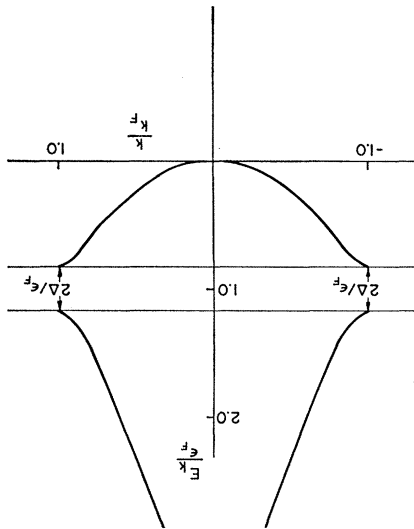


FIG. 1. The electron-dispersion relations for the valence (—) and conduction (---) band energies, given by Eq. (2.4).

band frequency. It is these transitions which we will describe within our model for the semiconductor at temperature  $T=0$ .

In Refs. 2 and 3, the properties of the dielectric constant are dealt with mainly through an analysis of the different contributions to the various sum rules which the imaginary and real parts of  $\epsilon(\mathbf{q}, \omega)$  must satisfy. The convenience of this method is that none of the details of the Bloch functions need to be investigated, because the individual oscillator strengths are not required. These authors considered the sum rules and rely on an interpretation and fitting of the data in terms of them to determine in which regions of  $\omega$  the various transitions play the most important role in obtaining a value of  $\epsilon(\mathbf{q}, \omega)$ . In order to explain the data they find it necessary to introduce a finite band-state lifetime which is taken for simplicity to depend only on the band indices and not on the energies of the states. The magnitudes of the lifetimes ( $10^{-15}$  sec) needed in this rough calculation are characteristic of those expected from electron-electron, rather than from electron-phonon interactions.

The aims of our work on semiconductors are quite different. We propose to explore systematically the dielectric constant for a particular model of a semiconductor including, as suggested by previous calculations,<sup>3</sup> the interactions between electrons but ignoring electron-phonon interactions. It should be noted that the interaction between electrons is Coulombic, and thus longitudinal, while the incident electron-phonon coupling is transverse. However, in the optical limit, ( $\mathbf{q} \rightarrow 0$ ), the distinction between the two disappears. For our model we use a three-dimensional extension of the nearly-free-electron gas model, which Penn<sup>5</sup> has employed in his discussion of the static dielectric constant. We first consider the polarization which would result if particles

<sup>5</sup> David R. Penn, Phys. Rev. **128**, 2093 (1962).

propagated freely and determine the resultant optical absorption  $\epsilon_2(\mathbf{q} \rightarrow 0, \omega)$ . This is done in Sec. II. By formulating the calculation field-theoretically we set up a convenient perturbation expansion, representable by Feynman diagrams. For simplicity this is done at  $T=0^\circ\text{K}$ ; finite temperature corrections should become important only when  $T$  becomes of the order of the gap energy, which is typically several volts. We are then able to consider in detail the various many-body effects which alter the above unperturbed calculation of  $\epsilon(\omega)$ .

These many-body effects are of two distinct types. The first is discussed in Sec. III and involves the introduction of a self-energy in the previously free-particle-type propagators. This is not a simple constant lifetime, but rather a frequency-dependent self-energy resulting from the possibility of the initial electron-hole pair which was created by the external field creating subsequent electron-hole pairs as a result of scattering off the particles in the Fermi sea. The importance of this effect and the shortcomings of the constant lifetime approximation of the previously cited references are discussed in this section. The second type of many-body effect we consider (Sec. IV) involves the scattering against each other of the initially created polarization pair. These effects are in the nature of corrections to the polarization vertices and approximate values for these corrections are obtained.

As we have mentioned above, our explicit calculations of self-energy and vertex corrections to  $\epsilon(\omega)$  require a model for the semiconductor. It is true that the model is simple and cannot be said to describe realistically the broad class of diamond structure semiconductors we consider. However, what we are mainly concerned with are the many-body effects reflected in  $\epsilon_2(\omega)$ . The possibility of sorting these out experimentally arises from the observed weak dependence of  $\epsilon(\omega)$  on the details of the band structure at photon energies  $\omega$  greater than about 5 eV. In particular, peaks reflecting singularities in the joint band density of states disappear above this energy, and the rate of the monotonic decrease of  $\epsilon_2$  with  $\omega$  is the feature which the sum rules and constant lifetime approximations have been invoked to explain. We therefore work within the framework of one model and show how the two effects discussed above alter the simplest calculation of  $\epsilon_2(\omega)$  based on this model. We find that the self-energy and vertex corrections significantly raise  $\epsilon_2(\omega)$  above the unperturbed value,  $\epsilon_0(\omega)$ . The net effect is to bring the calculated  $\epsilon_2(\omega)$  closer to the experimentally observed one. We believe that different, more complicated choices of model would show the same qualitative enhancements of  $\epsilon_2(\omega)$ . Results, conclusions, and limitations are discussed in Sec. V.

## II. (a) The Potential Model

For the one-dimensional crystal, we expand the lattice potential, as usual, in a Fourier series,

$$V(x) = \sum_K V_K e^{iKx}. \quad (2.1)$$

The  $K$ 's appearing are the wave vectors of the reciprocal lattice, the smallest of which has magnitude  $2k_F$ . Since we are considering an intrinsic semiconductor characterized by a single valence band, the quantity  $k_F$  is identical to the Fermi wave vector. In the absence of the potential (2.1), the unperturbed electrons are described by plane waves. The introduction of the lattice potential distorts primarily those plane waves having  $k$  values near  $k_F$ , modifying them most strongly through the  $K = 2k_F$  component of the potential. We denote this coefficient by  $\Delta$ .

The isotropic extension of this model to three dimensions consists of the perturbation's mixing the state  $\mathbf{k}$  with  $\mathbf{k} + \mathbf{K}$ , the vector  $\mathbf{K}$  having magnitude  $2k_F$  and direction opposite to that of  $\mathbf{k}$ . First-order perturbation theory gives the nearly-free-electron wave functions for the conduction (denoted by  $+$ ) and valence ( $-$ ) bands,

$$\psi_{\mathbf{k}}^{\pm}(\mathbf{r}) = (1 + (\alpha_{\mathbf{k}}^{\pm})^2)^{-1/2} (e^{i\mathbf{k}\cdot\mathbf{r}} + \alpha_{\mathbf{k}}^{\pm} e^{i(\mathbf{k}+\mathbf{K})\cdot\mathbf{r}}), \quad (2.2)$$

where

$$\alpha_{\mathbf{k}}^{\pm} = \frac{1}{2\Delta} \{ \epsilon_{\mathbf{k}+\mathbf{K}} - \epsilon_{\mathbf{k}} \pm [(\epsilon_{\mathbf{k}+\mathbf{K}} - \epsilon_{\mathbf{k}})^2 + 4\Delta^2]^{1/2} \}. \quad (2.3)$$

The quantities  $\epsilon_{\mathbf{k}}$  are the unperturbed plane wave energies measured with respect to the Fermi surface  $\epsilon_F$  in terms of which the valence and conduction-band energies are given by

$$E_{\mathbf{k}}^{\pm} = \frac{1}{2} \{ \epsilon_{\mathbf{k}} + \epsilon_{\mathbf{k}+\mathbf{K}} \pm [(\epsilon_{\mathbf{k}+\mathbf{K}} - \epsilon_{\mathbf{k}})^2 + 4\Delta^2]^{1/2} \}. \quad (2.4)$$

Throughout we will work within the reduced zone scheme so that in all of the above expressions  $k$  always has magnitude less than  $k_F$ . The electron dispersion relation for this two-band semiconductor is shown in Fig. 1.

For the optical (long-wavelength) limit at finite frequencies only the interband, i.e., umklapp, transitions contribute to the imaginary part of the dielectric constant,  $\epsilon_2(\mathbf{q} \rightarrow 0, \omega)$ . These transitions are induced by the external field component  $v_{\mathbf{q}} \exp(i\mathbf{q}\cdot\mathbf{r})$ , through the interaction

$$V_{\text{ext}}(\mathbf{q}) = \int d^3r \sum_{\substack{\mathbf{p}, \mathbf{p}' \\ (\text{1st B.Z.})}} \{ c_{\mathbf{p}+\mathbf{K}}^+ \psi_{\mathbf{p}}^{-*}(\mathbf{r}) + c_{\mathbf{p}+\mathbf{K}}^+ \psi_{\mathbf{p}}^{+*}(\mathbf{r}) \} \{ c_{\mathbf{p}'} \psi_{\mathbf{p}'}^-(\mathbf{r}) + c_{\mathbf{p}'+\mathbf{K}} \psi_{\mathbf{p}'}^+(\mathbf{r}) \} v_{\mathbf{q}} e^{i\mathbf{q}\cdot\mathbf{r}}, \quad (2.5)$$

where  $c_{\mathbf{p}}^+$  is the second-quantized Fermion operator creating a nearly free electron with wave vector  $\mathbf{p}$ , and B.Z. stands for Brillouin zone. The result of the  $r$  integration in (2.5) is

$$V_{\text{ext}}(\mathbf{q}) = v_{\mathbf{q}} \sum_{\substack{\mathbf{p} \\ (\text{1st B.Z.})}} \left\{ c_{\mathbf{p}+\mathbf{K}}^+ c_{\mathbf{p}} \frac{1}{[1 + (\alpha_{\mathbf{p}}^+)^2]^{1/2}} \left[ \frac{1}{[1 + (\alpha_{\mathbf{p}-\mathbf{q}}^-)^2]^{1/2}} - \frac{\alpha_{\mathbf{p}}^+ \alpha_{\mathbf{q}}^+}{[1 + (\alpha_{\mathbf{q}}^+)^2]^{1/2}} \right] \right. \\ \left. + c_{\mathbf{p}}^+ c_{\mathbf{p}+\mathbf{K}} \frac{1}{[1 + (\alpha_{\mathbf{p}}^-)^2]^{1/2}} \left[ \frac{1}{[1 + (\alpha_{\mathbf{p}-\mathbf{q}}^+)^2]^{1/2}} - \frac{\alpha_{\mathbf{p}}^- \alpha_{\mathbf{q}}^-}{[1 + (\alpha_{\mathbf{q}}^-)^2]^{1/2}} \right] + c_{\mathbf{p}}^+ c_{\mathbf{p}-\mathbf{q}} + c_{\mathbf{p}+\mathbf{K}}^+ c_{(\mathbf{p}-\mathbf{q})+\mathbf{K}} \right\}, \quad (2.6)$$

where

$$\mathbf{k} = [\mathbf{p} - 2k_F(\mathbf{p}/p) - \mathbf{q}] + \mathbf{K}. \quad (2.7)$$

The interparticle interaction is also Coulombic and can be written as

$$V_{\text{int}} = \sum_{\mathbf{q}} v_{\mathbf{q}} \frac{V_{\text{ext}}(\mathbf{q}) V_{\text{ext}}(-\mathbf{q})}{v_{\mathbf{q}} v_{\mathbf{q}}}. \quad (2.8)$$

We see that as in Eq. (2.5) the bare interaction,  $v_{\mathbf{q}} = 4\pi e^2/q^2$ , is modified by factors expressing the coupling between initial and final states. The presence of these factors in (2.8) will be made obvious in the next section.

### (b) Infinite-Lifetime Calculation

The main purpose of this paper is to exhibit the effects of the interparticle Coulomb interactions on  $\epsilon_2(\mathbf{q} \rightarrow 0, \omega)$ . Preparatory to doing this, we consider  $\epsilon_2(\omega)$  in the absence of these interactions; i.e., in the case where the single-particle excitations are infinitely long-lived.

Within the random phase approximation the complex dielectric constant is given by<sup>4</sup>

$$\epsilon(\mathbf{q}, \omega) = 1 + v_{\mathbf{q}} \Pi(\mathbf{q}, \omega) = 1 + 4\pi\alpha(\mathbf{q}, \omega), \quad (2.9)$$

where  $\alpha(\mathbf{q}, \omega)$  is the complex polarizability. This equation is expressed schematically in Fig. 2, where the irreducible polarization,  $\Pi(\mathbf{q}, \omega)$ , is the sum of all Feynman diagrams containing two external vertices

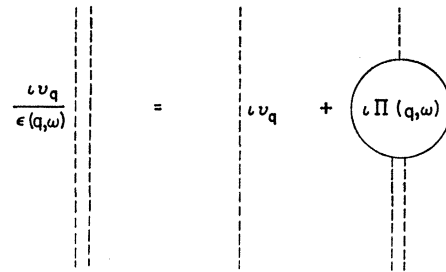


FIG. 2. The equation for the complex dielectric constant, given (within the RPA) by Eq. (2.9).

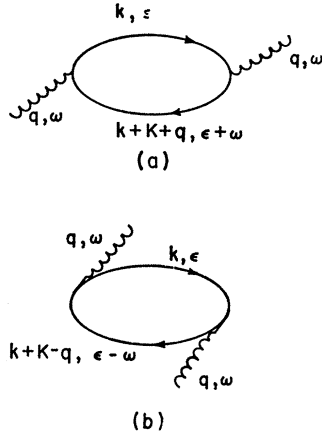


FIG. 3. Lowest order diagrams contributing to the irreducible polarizability,  $\Pi(\mathbf{q}, \omega)$ . Figures 3(a) and 3(b) differ by the order of the absorption and emission processes for the photon.

which cannot be split into two parts by cutting a single interaction line. For our problem the electron and hole propagators in these Feynman diagrams represent nearly-free-particle states with the coupling factors of Eq. (2.8) associated with the vertices rather than with the interaction lines.

The lowest order diagrams contributing to  $\Pi(\mathbf{q}, \omega)$  are shown in Fig. 3. The presence of the two coupling factors in (2.8) is now clear. The change of sign in the value of  $\mathbf{q}$  appearing in the two factors corresponds to the photon producing the electron-hole pair being absorbed at one vertex and emitted at the other. The propagators in this diagram are given by

$$G^\pm(\mathbf{p}, \omega) = [\omega - E_{p^\pm}(1 - i\eta)]^{-1}, \quad (2.10)$$

where  $\eta = 0^+$ . The  $E_{p^\pm}$ 's are just the almost-free-electron values of Eq. (2.4). The contribution of Fig. 3 to the polarization,  $\Pi(\mathbf{q}, \omega)$ , is therefore

$$-i\Pi_0(\mathbf{q}, \omega) = \frac{2}{(2\pi)^4} \int d^3p \int d\epsilon 2f(\mathbf{p}, \mathbf{q}) \times (\epsilon - E_{p+K} + i\eta)^{-1} (\epsilon - \omega - E_{p-q} - i\eta)^{-1}, \quad (2.11)$$

where the multiplicative factor of two results from a sum over spins and the wave vectors  $\mathbf{p}$  are restricted to lie within the Fermi sphere. The quantity  $f(\mathbf{p}, \mathbf{q})$  represents

$$f(y) \equiv \lim_{q \rightarrow 0} f(\mathbf{p}, \mathbf{q})/q^2 = (\epsilon_F/\Delta)^2 [1 + (2\epsilon_F/\Delta)^2 (1-y)^2]^{-2} \cos^2(\mathbf{q}, \mathbf{p}) k_F^{-2}. \quad (2.14)$$

We can then write (2.13) in the long-wavelength limit as

$$\begin{aligned} \epsilon_2(\omega) &= \frac{16}{3a_0 k_F} (\epsilon_F/2\Delta)^2 [1 - (4\Delta^2/\omega^2)]^{-1/2} \int_0^1 dy y^2 \delta[y - 1 + (\omega^2 - 4\Delta^2)^{1/2}/4\epsilon_F] [1 + (4\epsilon_F^2/\Delta^2)(1-y)^2]^{-2} \\ &= \frac{16}{3a_0 k_F} (\epsilon_F/2\Delta)^2 (2\Delta/\omega)^4 \frac{\omega}{(\omega^2 - 4\Delta^2)^{1/2}} [1 - ((\omega/4\epsilon_F)^2 - (\Delta/2\epsilon_F)^2)^{1/2}]^2, \end{aligned} \quad (2.15)$$

where  $a_0$  is the Bohr radius,  $a_0 = 1/me^2$ . At this point we may use this expression to obtain numerical results for  $\epsilon_2(\omega)$  in the absence of the many-body effects to be described in the next section. The relevant parameter of Eq.

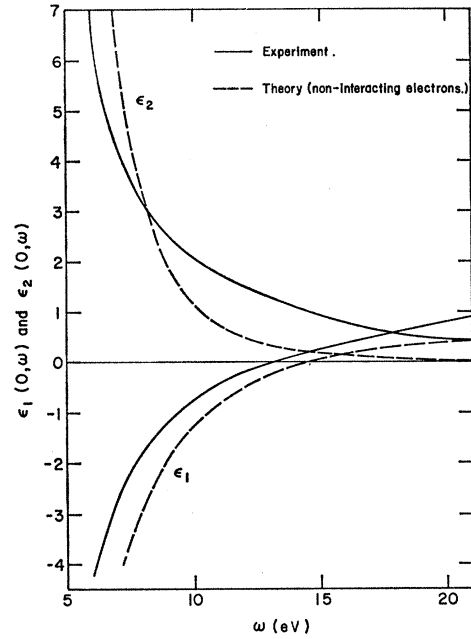


FIG. 4. The real and imaginary parts of the dielectric constant,  $\epsilon(q \rightarrow 0, \omega) = \epsilon_1(\omega) + i\epsilon_2(\omega)$ , for Ge, as measured optically (solid curves) and as predicted by the theory of noninteracting electrons of Sec. II (dashed curves), Eqs. (2.15) and (2.20).

the coupling at the two vertices and is given by

$$2f(\mathbf{p}, \mathbf{q}) = [1 + (\alpha_p^+)^2]^{-1} \{ [1 + (\alpha_{p-q}^-)^2]^{-1/2} + [1 + (\alpha_k^-)^2]^{-1/2} \alpha_p^+ \alpha_k^- \}^2 + [1 + (\alpha_p^-)^2]^{-1} \times \{ [1 + (\alpha_{p-q}^+)^2]^{-1/2} + [1 + (\alpha_k^+)^2]^{-1/2} \alpha_p^- \alpha_k^+ \}^2, \quad (2.12)$$

with  $k$  defined by Eq. (2.7). The two terms in (2.12) correspond to the two graphs of Fig. 3. Doing the  $\epsilon$  integration in (2.11) and using the definition (2.9), we obtain for the imaginary part of the dielectric constant,

$$\epsilon_2(\mathbf{q}, \omega) = \frac{2v_q}{(2\pi)^2} \int d^3p f(\mathbf{p}, \mathbf{q}) \delta(\omega + E_{p-q} - E_{p+K}). \quad (2.13)$$

Using Eqs. (2.3) and (2.4) in the  $q \rightarrow 0$  limit and introducing the dimensionless variable  $y = p/k_F$  we find

(2.15) is the ratio  $(2\Delta/\epsilon_F)$ . This could be obtained by matching Eq. (2.15) with an experimental point. In fact, Penn,<sup>5</sup> who has used this model, matches his expression for the static value  $\epsilon(0,0)$ , to obtain  $(2\Delta/\epsilon_F)=0.36$  in the case of Ge. To make our work consistent with his, we also choose this value of  $(2\Delta/\epsilon_F)$ . The results are shown in Fig. 4, where we have taken  $a_0k_F=0.92$ , the value appropriate to four free electrons per atom at the atomic density of Ge. In the following sections we take all energies and momenta in units of  $\epsilon_F$  and  $k_F$ , respectively. We find that this curve falls off much too rapidly with  $\omega$  when compared with the results of Ref. 3. This decrease arises both from the falloff in the joint density of states and from the reduced interband coupling by the static lattice as band states separated by progressively higher energies contribute. In the next two sections we will see how self-energy and vertex corrections serve to bring about a more gradual decrease with  $\omega$ , lifting the theoretical curve nearer the experimental one.

We can also calculate—at least approximately—the real part of the dielectric constant,  $\epsilon_1$ , within the infinite lifetime approximation. From Eqs. (2.9), (2.11), and (2.14) we have

$$\epsilon_1(q \rightarrow 0, \omega) = 1 - \frac{4e^2}{3\pi\Delta^2} P \int_0^1 dk \frac{k^2}{\omega + E_k - E_{k+K}} [1 + (2/\Delta)^2(1-k)^2]^{-2}, \quad (2.16)$$

where  $P$  denotes the principal value of the integral. The substitution  $x = (2/\Delta)(k-1)$  puts the integral into the form

$$\frac{\Delta}{2} P \int_{-2/\Delta}^0 dx \frac{(\Delta/2)^2 x^2 + \Delta x + 1}{\omega - 2\Delta(1+x^2)^{1/2}} (1+x^2)^{-2} = \frac{\Delta}{2\omega} P \int_{-\tan^{-1}2/\Delta}^0 d\theta \frac{[(\Delta/2)^2 \tan^2\theta + \Delta \tan\theta + 1] \cos^5\theta}{\cos\theta - 2\Delta/\omega}. \quad (2.17)$$

This is now in the form of a sum of standard integrals, and after some algebraic manipulations we find for  $\omega > 2\Delta$

$$\begin{aligned} \epsilon_1(\omega) = 1 - \frac{e^2}{3\pi\Delta^2} \rho \left\{ (\Delta^2/8) \tan^{-1}(2/\Delta) + (3/8)\delta \tan^{-1}(2/\Delta) + \delta\gamma^2/\Delta \right. \\ + (\delta\gamma^2/8\Delta)(2\gamma^2-1) - (\Delta/4)(1-\gamma^4) + \rho[\Delta\gamma/2 + (2\delta\gamma/3\Delta)(\gamma^2+2) - (\Delta/3)(1-\gamma^3)] \\ + \rho^2[(\Delta/2)^2 \tan^{-1}(2/\Delta) + (\delta/2)[\tan^{-1}(2/\Delta) + \gamma^2/\Delta] - (\Delta/2)(1-\gamma^2)] + \rho^3[2\delta\gamma/\Delta - \Delta(1-\gamma)] \\ \left. + \rho^4[\delta \tan^{-1}(2/\Delta)] + (1-\rho^2)^{-1/2}[(\Delta/2)^2\rho^3 + (1-\Delta^2/4)\rho^5] \ln \left| \frac{(1-\rho^2)^{1/2} \tan[\frac{1}{2} \tan^{-1}(2/\Delta)] + 1 - \rho}{(1-\rho^2)^{1/2} \tan[\frac{1}{2} \tan^{-1}(2/\Delta)] - 1 + \rho} \right| \right. \\ \left. - \Delta\rho^4 \ln \left| \frac{1-\rho}{\rho-\gamma} \right| \right\}, \quad (<1) \quad (2.18) \end{aligned}$$

where we have used for frequently occurring constants the symbols

$$\rho = 2\Delta/\omega; \quad \delta = 1 - \Delta^2/4; \quad \gamma = (1 + \Delta^2/4)^{-1/2}. \quad (2.19)$$

For the values of  $\Delta$  and  $k_F$  that we have taken to describe Ge this becomes

$$\begin{aligned} \epsilon_1(\omega) = 1 - 0.068\rho + 0.076\rho^2 + 0.086\rho^3 + 0.102\rho^4 + 0.182\rho^5 \\ + (1-\rho^2)^{-1/2}(0.0060\rho^4 + 0.496\rho^5) \ln \left| \frac{0.713(1-\rho^2)^{1/2} + 1 - \rho}{0.713(1-\rho^2)^{1/2} - 1 + \rho} \right| - 0.022\rho^4 \ln \left| \frac{1-\rho}{\rho-0.089} \right|. \quad (2.20) \end{aligned}$$

This is also compared with the experimental values for Ge in Fig. 4.

### III. SELF-ENERGY EFFECTS

A single electron introduced into the conduction band at an energy less than  $2\Delta$  above the band minimum will remain in that state, since the minimum excitation energy for the filled valence band ( $2\Delta$ ) is not available. A similar statement can be made for a single hole in the valence band. However, at the higher optical excitation energies in which we are interested, electrons and/or holes are readily able to scatter by Coulomb interactions so as to conserve both the energy and momentum of the system. In a simple single-particle picture the results of this scattering can be described in terms of the lifetimes of the states, but more generally it is necessary to deal with the electron and hole self-energies in the many-body system. In particular, we want to consider optical

absorption as proceeding in two steps—an optical transition to an energy-nonconserving intermediate state, then scattering via the interparticle Coulomb interactions to the final state. We first ignore interactions between the initially created electron-hole pair and investigate the effects of the interaction of each with the rest of the system. The Green's function  $G(\mathbf{p}, \omega)$  describing particle (or hole) propagation in the semiconductor, is related to the corresponding propagator in a noninteracting system  $G_0(\mathbf{p}, \omega)$ , by the Dyson equation<sup>6</sup>

$$G(\mathbf{p}, \omega) = G_0(\mathbf{p}, \omega) + G_0(\mathbf{p}, \omega) \Sigma(\mathbf{p}, \omega) G(\mathbf{p}, \omega). \quad (3.1)$$

As is clear from the iterative solution of this equation, the irreducible self-energy  $\Sigma(\mathbf{p}, \omega)$  describes all processes the system can undergo, starting from and ending with a freely propagating excitation  $(\mathbf{p}, \omega)$ , without at any intermediate point returning to that state. The resultant  $G(\mathbf{p}, \omega)$  thus contains just those effects we have proposed to include at this point. If  $\Sigma(\mathbf{p}, \omega)$  is frequency-independent, then propagation in time, as given by

$$\begin{aligned} G(\mathbf{p}, t) &= \int \frac{d\omega}{2\pi} \frac{1}{G_0^{-1}(\mathbf{p}, \omega) - \Sigma(\mathbf{p})} e^{-i\omega t} = \int \frac{d\omega}{2\pi} \frac{e^{-i\omega t}}{\omega - E_p - \text{Re}\Sigma - i \text{Im}\Sigma} \\ &= i e^{-i(E_p + \text{Re}\Sigma)t} e^{(\text{Im}\Sigma)t}, \quad \text{if } t > 0 \text{ and } E_p + \text{Re}\Sigma > 0 \text{ or, } t < 0 \text{ and } E_p + \text{Re}\Sigma < 0, \\ &0 \quad \text{otherwise,} \end{aligned} \quad (3.2)$$

is describable in terms of exponential decay, with a lifetime  $\tau = |\text{Im}\Sigma|^{-1}$ . In general, this is not the case; but it is still true that the feature of central importance for us—that is, the fact that the occupation of a single-band state does not represent an eigenstate of the system, but rather a linear combination of eigenstates with various energies—is manifested by a nonvanishing imaginary part of the self-energy.

The physical interpretation (as well as the mathematics of the calculation) is simplest if the appropriate quantities are written in a spectral representation. As in the previous section, we want to calculate the irreducible polarizability,  $\Pi$ , with the present approximation consisting of replacing the bare propagators  $G_0$  by more accurate Green's functions  $G$  (the diagram is the same, with this new interpretation of the lines). The analytic continuation of  $G(\mathbf{p}, \omega)$  into the complex  $\omega$  plane is conveniently written in the form of a dispersion integral

$$G(\mathbf{p}, \omega) = \int_{-\infty}^{\infty} \frac{A(\mathbf{p}, \nu) d\nu}{\omega - \nu} \frac{1}{2\pi}. \quad (3.3)$$

The spectral weight function  $A(\mathbf{p}, \nu)$  is given by

$$(2\pi)^{-1} A(\mathbf{p}, \nu) = \sum_m |\langle m | c_p | +0 \rangle|^2 \delta(\nu - \omega_{m0}^{N+1}) + \sum_m |\langle m | c_p | 0 \rangle|^2 \delta(\nu - \omega_{m0}^{N-1}) \quad (3.4)$$

describing the density of eigenstates of excitation energy  $\nu$  (and momentum  $\mathbf{p}$ ) in the state produced by the addition of one-conduction-band electron  $\mathbf{p}$  to the ground state  $|0\rangle$ . (The energy of the exact eigenstate  $|m\rangle$ , referred to that of the ground state, is  $\omega_{m0}$ .) This is thus a convenient means for obtaining expressions for the polarizability or dielectric constant directly in terms of the density of states available for the various scattering processes. The physical Green's functions are to be evaluated always at frequencies infinitesimally removed from the real axis in the first and third quadrants (so that particle states exponentially decay, rather than grow at large positive times). Then, in particular, we have

$$\begin{aligned} \lim_{q \rightarrow 0} -iv_q \Pi(\omega, q) &= 8\pi e^2 \int \frac{d^3 \mathbf{p}}{(2\pi)^3} f(\mathbf{p}) \int \frac{d\epsilon}{2\pi} G(\mathbf{p}, \epsilon - \omega) G(\mathbf{p} + \mathbf{K}, \epsilon) \\ &= \frac{8\pi e^2}{(2\pi)^6} \int d^3 \mathbf{p} f(\mathbf{p}) \int_{-\infty}^{\infty} d\epsilon \int_{-\infty}^{\infty} d\nu \int_{-\infty}^{\infty} d\nu' \frac{A(\mathbf{p}, \nu)}{\epsilon - \omega + i\eta\nu - \nu} \left[ \frac{A(\mathbf{p} + \mathbf{K}, \nu')}{\epsilon + i\eta\nu' - \nu'} \right] \\ &= \frac{8\pi e^2 i}{(2\pi)^6} \int d^3 \mathbf{p} f(\mathbf{p}) \left\{ \int_0^{\infty} d\nu \int_{-\infty}^0 d\nu' + \int_{-\infty}^0 d\nu \int_0^{\infty} d\nu' \right\} \frac{A(\mathbf{p}, \nu) A(\mathbf{p} + \mathbf{K}, \nu')}{\omega + \nu - \nu' + i\eta}, \end{aligned} \quad (3.5)$$

<sup>6</sup> For a thorough discussion of the Dyson equation and many-body field-theoretic methods in general, see A. A. Abrikosov, L. P. Gorkov, and I. E. Dzyaloshinski, *Methods of Quantum Field Theory in Statistical Physics* (Prentice-Hall, Inc., Englewood Cliffs, New Jersey, 1963).

where, as before,  $\eta=0^+$ . By Eq. (2.9) the real part of this expression gives  $\epsilon_2(\omega)$  itself (within the present approximation for  $\Pi$ ), and we find the readily interpreted result:

$$\epsilon_2(\omega) = \frac{e^2}{4\pi^3} \int d^3p 2f(p) \int_0^\omega A(p, \nu - \omega) A(p+K, \nu) d\nu. \quad (3.6)$$

Thus, an initial electron-hole pair is created at  $p, p+K$ , each of these then scattering from the rest of the system to produce excitations of energies  $\nu$  and  $\omega - \nu$ , respectively. The limits on the  $\nu$  integral simply ensure that the state associated with  $p+K$  is indeed a particle ( $\nu \geq 0$ ) and that the one associated with  $p$  is a hole ( $\nu - \omega \leq 0$ ). We have seen that the noninteracting-electron results lead to an absorption which falls off too rapidly at large  $\omega$ . This was observed to be a result largely of the rapid decrease of interband coupling [the factor  $f(p)$ ], as one moved away from the gap region. We now see that if interactions lead to appreciable spectral weight at high energies for momenta  $p$  near unity (the gap edge) the predicted high- $\omega$  absorption may be suitably increased. In the corresponding processes the initial pair would be created in an intermediate state well off the energy shell and would scatter against the remaining particles to produce a multiple-pair high-energy final state. The spectral weight function is just the density of such states.

The inadequacies of the constant-lifetime approximation are now apparent. The low-energy single-particle excitations which should find it difficult or impossible to decay because of the presence of the energy gap are assigned lifetimes as short as those of high-energy excitations. A more realistic assignment of lifetimes to band states, however, although more satisfactory is still insufficient. The shortest lifetimes (and therefore the largest changes in spectral weight) must be associated with the highest energy excitations, where the greatly reduced oscillator strengths minimize the magnitude of the final effect on  $\epsilon_2(\omega)$ . Furthermore, redistribution of spectral weight at one momentum tends to be compensated by that at another [e.g., reduction of the  $\delta$  function at the band energy  $\omega = E_p$  in  $A(p, \omega)$  is in part made up by the tails of  $A(p', \omega)$  for all other  $p'$  at  $\omega = E_p$ ]. In short, it is necessary to introduce spectral weight at high energies in a region of momentum space ( $p \approx 1$ ) where the oscillator strength is large enough to affect appreciably the absorption probability—and thus  $\epsilon_2(\omega)$ . It is therefore essential to estimate the behavior of the full self-energy function, including its explicit dependence on frequency.

The central problem is then the evaluation of  $\Sigma(p, \omega)$ . From the spectral representation of  $G(p, \omega)$  [Eq. (3.3)] we see that

$$A(p, \nu) = 2 \text{Im} G(p, \nu - i\eta). \quad (3.7)$$

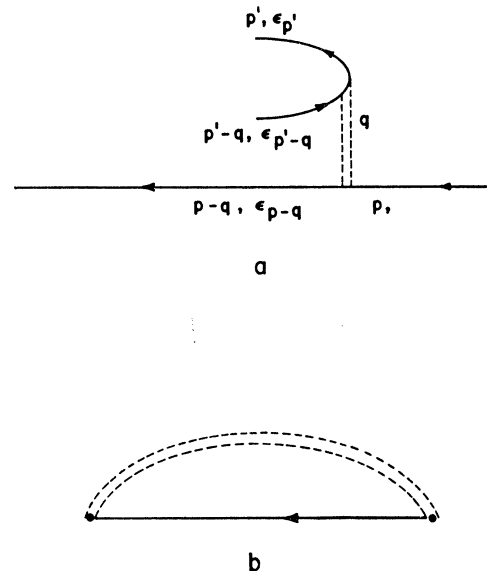


FIG. 5. Figure 5(a) illustrates the Auger-type processes leading to the self-energy diagram of Fig. 5(b), the double dashed line being the screened Coulomb interaction.

In terms of the self-energy this becomes

$$A(p, \nu) = \frac{2 \text{Im} \Sigma(p, \nu)}{(\nu - \text{Re} \Sigma - E_p)^2 + (\text{Im} \Sigma)^2}. \quad (3.8)$$

It is the deviation of  $\text{Im} \Sigma$  from an infinitesimal which signals the presence of "lifetime" effects. The real part of the self-energy essentially shifts the band energies  $E_p$  to  $E_{p'} = E_p + \text{Re} \Sigma(p, E_{p'})$ . We make the approximation that this is primarily just a rigid-band shift [ $\text{Re} \Sigma(p, E_{p'})$  independent of  $p$ ], and other estimates<sup>7</sup> indicate that this is probably very nearly true in real crystals (renormalization effects, represented by the frequency dependence of  $\text{Re} \Sigma$ , will be discussed later). We then proceed to calculate the imaginary part of  $\Sigma$ , representing the possibility for the single-particle ( $p, \omega$ ) to scatter against the filled valence band so as to produce a final state of energy  $\omega$  with all particles on the energy shell.

We suggest that the dominant scattering process for a high-energy conduction electron is the simplest one—an Auger-type effect. The first electron interacts by a screened Coulomb potential with the filled band, kicking a valence electron up to the conduction band and leaving a second hole in the valence band. For a real absorption process both electrons and both holes must be on the energy shell (each has the band energy  $E_p$  appropriate to its momentum  $p$ ). The process is illustrated diagrammatically in Fig. 5(a) and the corresponding self-energy diagram is shown in Fig. 5(b). The screening should be adequately accounted for by the random-phase approximation<sup>4</sup> (the calculation of Sec. II, but for

<sup>7</sup> That this approximation is valid for Si has been demonstrated by an explicit band calculation by E. O. Kane, Phys. Rev. 146, 558 (1966).

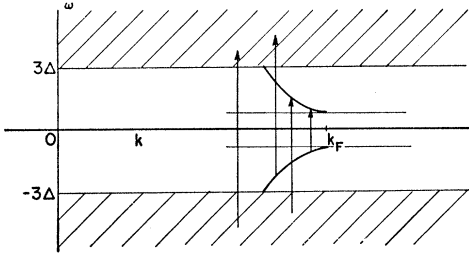


FIG. 6. The regions in momentum-energy space accessible as final states through the types of scattering processes considered. A continuum now exists for  $|\omega| < 3\Delta$ , while only the original band states exist for  $|\omega| > 3\Delta$ . The arrows indicate the various kinds of transitions which can occur.

general  $q$ ), but even with this simplification a straightforward determination of  $\Sigma$  is extremely difficult. Instead of proceeding directly at this point, we take advantage of the fact that particles of energy much greater than  $2\Delta$  will be essentially unaware of the existence of the gap, and we therefore expect  $\text{Im}\Sigma(p, \omega)$  for these high values of  $\omega$  to be the same as it would be in a free-electron gas of the same density as the valence electrons in the semiconductor. This simpler calculation has been made.<sup>8</sup> We know further that in the semiconductor,  $\text{Im}\Sigma(\omega) = 0$  for  $|\omega| < 3\Delta$ , so we suggest a reasonable interpolation between the value zero at  $|\omega| = 3\Delta$  and the asymptotic form obtained from the free-electron-gas calculation as a sensible approximation for  $\text{Im}\Sigma(p, \omega)$ . Certainly the general features and correct orders of magnitude of self-energy effects should be exhibited by such an approximation. In a previous calculation<sup>8</sup> we showed that  $\text{Im}\Sigma(p, \omega)$  in the free-electron gas depends

importantly only on the frequency variable. Furthermore, for energies up to several times the Fermi energy, the frequency dependence was found to be monotonic and could be rather closely approximated by a quadratic function:  $\Sigma(p, \nu) \approx \alpha \nu^2 \text{sgn}(\nu)$  independent of  $p$ . As an interpolation for the semiconductor we have chosen a form with which we can conveniently calculate:

$$\begin{aligned} \text{Im}\Sigma(p, \nu) &= \alpha(\nu + 3\Delta)^2, & \nu \leq -3\Delta \\ &= \eta, & -3\Delta \leq \nu < 0 \\ &= -\eta, & 0 < \nu \leq 3\Delta \\ &= -\alpha(\nu - 3\Delta)^2, & \nu \geq 3\Delta. \end{aligned} \quad (3.9)$$

Since  $\text{Re}\Sigma$  represents primarily just a shift of the zero of energy we take  $\text{Re}\Sigma \approx 0$ . Substitution of Eq. (3.9) into (3.8) then gives the spectral weight functions to be used in Eq. (3.6) to find  $\epsilon_2(\omega)$ , as corrected for self-energy effects. The regions in momentum-energy space where there is spectral weight (those regions accessible as final states through the types of scattering processes we have considered) are shown in Fig. 6. We have indicated the original band states of energy  $|\nu| < 3\Delta$ , which are still good eigenstates in this approximation [ $A(p, \omega) = 2\pi\delta(\omega - E_p)$  along these curves]. There is, in addition, a continuum of available states for  $|\nu| > 3\Delta$  at all momenta  $p$ . There are no effects on  $\epsilon_2(\omega)$  for photon energy  $\omega < 4\Delta$ , since both electron and hole states are infinitely long-lived here [note that  $A(p, \nu - \omega)$  and  $A(p + K, \nu)$  are both  $\delta$  functions in Eq. (3.6) for  $\omega < 4\Delta$ ]. Transitions between valence and conduction continua can occur only if  $\omega > 6\Delta$ . Between these limits,  $4\Delta < \omega < 6\Delta$ , Eq. (3.6) becomes

$$\begin{aligned} \epsilon_2(\omega) = \frac{e^2}{4\pi^3} \int d^3p f(p) \left\{ \int_{-\Delta}^{\omega-3\Delta} d\nu \frac{2\alpha(\nu - \omega + 3\Delta)^2}{(\nu - \omega - E_p)^2 + \alpha^2(\nu - \omega + 3\Delta)^4} (2\pi)\delta(\nu - E_{p+K}) \right. \\ \left. + \int_{\omega-3\Delta}^{3\Delta} d\nu (2\pi)\delta(\nu - \omega - E_p) (2\pi)\delta(\nu - E_{p+K}) \right. \\ \left. + \int_{3\Delta}^{\omega} d\nu (2\pi)\delta(\nu - \omega - E_p) \frac{2\alpha(\nu - 3\Delta)^2}{(\nu - E_{p+K})^2 + \alpha^2(\nu - 3\Delta)^4} \right\}, \quad 4\Delta \leq \omega \leq 6\Delta. \end{aligned} \quad (3.10)$$

The three terms within brackets, each the integral of a product of electron and hole spectral weight functions, are readily interpreted. We recall from Eq. (3.6) that the integration variable  $\nu$  represents the particle energy. Thus, the second term is the contribution from optical transitions between those valence band states  $p$  and the corresponding conduction band states  $p + K$  which are separated by precisely the right energy:  $E_{p+K} - E_p = \omega$ ; only a single value of  $|p|$  contributes. The first term represents transitions (always of the same energy  $\omega$ ) between the valence continuum at  $p$  and the conduction band. These processes are also illustrated in Fig. 6.

The frequency integrals are trivial, and the only dependence on the direction of  $p$  is found in the coupling factor  $f(p)$ . Then we can simplify Eq. (3.10) to

$$\begin{aligned} \epsilon_2(\omega) = \frac{4e^2}{\pi} \int_0^1 d\hat{p} \hat{p}^2 \bar{f}(\hat{p}) \left\{ \theta(\omega - 3\Delta - E_{p+K}) \frac{\alpha(E_{p+K} - \omega + 3\Delta)^2}{(E_{p+K} - \omega - E_p)^2 + \alpha^2(E_{p+K} - \omega + 3\Delta)^4} \right. \\ \left. + \pi\theta(3\Delta - E_{p+K})\delta(E_{p+K} - \omega - E_p) + \theta(3\Delta - \omega - E_p) \frac{\alpha(\omega + E_p - 3\Delta)^2}{(\omega + E_p - E_{p+K})^2 + \alpha^2(\omega + E_p - 3\Delta)^4} \right\}, \end{aligned} \quad (3.11)$$

<sup>8</sup> S. M. Bose, A. Bardasis, A. J. Glick, P. Longe, and D. Hone (to be published).

where  $\bar{f}(\boldsymbol{p})$  is the angular average of  $f(\boldsymbol{p})$  and  $\theta(\nu)$  is the unit step function

$$\begin{aligned}\theta(\nu) &= 1 & \text{if } \nu > 0 \\ &= 0 & \text{if } \nu < 0.\end{aligned}\quad (3.12)$$

This final integral over  $\boldsymbol{p}$  was carried out numerically on an IBM 7040 computer. Before discussing the numerical results, however, we complete the analysis by giving the corresponding solution for the frequency range  $\omega > 6\Delta$ :

$$\begin{aligned}\epsilon_2(\omega) &= \frac{e^2}{4\pi^3} \int d^3\boldsymbol{p} f(\boldsymbol{p}) \left\{ \int_{\Delta}^{3\Delta} d\nu \frac{2\alpha(\nu-\omega+3\Delta)^2}{(\nu-\omega-E_p)^2 + \alpha^2(\nu-\omega+3\Delta)^4} (2\pi)\delta(\nu-E_{p+K}) \right. \\ &\quad + \int_{3\Delta}^{\omega-3\Delta} d\nu \frac{4\alpha^2(\nu-\omega+3\Delta)^2(\nu+3\Delta)^2}{[(\nu-\omega-E_p)^2 + \alpha^2(\nu-\omega+3\Delta)^4][(\nu-E_{p+K})^2 + \alpha^2(\nu+3\Delta)^4]} \\ &\quad \left. + \int_{\omega-3\Delta}^{\omega} d\nu (2\pi)\delta(\nu-\omega-E_p) \frac{2\alpha(\nu-3\Delta)^2}{(\nu-E_{p+K})^2 + \alpha^2(\nu-3\Delta)^4} \right\}, \quad (\omega \geq 6\Delta). \quad (3.13)\end{aligned}$$

There are no longer pairs of electron-hole band states separated by these energies  $\omega$ , and the corresponding term in  $\epsilon_2(\omega)$  has disappeared. The new feature, as expected, is the presence of valence to conduction-continuum transitions, represented by the second term. This frequency integral is readily carried out by the use of partial-fraction techniques. The final integral over  $|\boldsymbol{p}|$  is again done numerically.

The quantitative results are presented in Fig. 7 and are compared with the corresponding curve for non-interacting electrons, calculated in Sec. II. The only new parameter characterizing self-energy effects is  $\alpha$ , the curvature of  $\text{Im}\Sigma(\omega)$ . This was chosen to give the best fit to  $\text{Im}\Sigma(\omega)$  for a free-electron gas of the density appropriate to the valence electrons of Ge. We found  $\alpha \approx \frac{1}{8}$ , with all energies taken, as usual, in units of  $\epsilon_F$ .

We should point out here that the approximation we have employed is not entirely consistent. In particular, the Kramers-Kronig relations connecting the real and imaginary parts of the self-energy are clearly not obeyed. Although  $\text{Re}\Sigma(\boldsymbol{p},\omega)$  leads to approximately a rigid-band shift on the energy shell ( $\omega = E_p$ ), it will not be independent of  $\omega$  for fixed  $\boldsymbol{p}$ . This must be taken into account if the density of states in  $k$  space is to be maintained correctly. The probability that the state  $c_{\boldsymbol{p}}^+|0\rangle$  contains an eigenstate of energy  $\omega$  [given by  $A(\boldsymbol{p},\omega)$ ], summed over all  $\omega$ , must be unity. Formally, a consistent treatment of  $\Sigma(\boldsymbol{p},\omega)$  must ensure satisfaction of the sum rule

$$\int_{-\infty}^{\infty} A(\boldsymbol{p},\omega) \frac{d\omega}{2\pi} = 1. \quad (3.14)$$

It is clear, in particular, that the frequency dependence of  $\text{Re}\Sigma$  does in fact renormalize the  $\delta$  functions in  $A(\boldsymbol{p},\omega)$  describing the band states: their weight is reduced from  $2\pi$  by a factor  $1/(1-\partial\Sigma/\partial\omega)$ . This will reduce band to band-state absorption somewhat, most strongly for  $E_p$  and  $E_{p+K}$  just below  $3\Delta$ . But for the regions of  $\boldsymbol{p}$  space important for the present calculation—namely, close to

the gap ( $\boldsymbol{p} \approx 1$ )—the total spectral weight in the continuum is small, and these renormalization effects are unimportant.

There are no substantial self-energy effects in  $\epsilon_2(\omega)$  until transitions between valence and conduction continua are allowed (at  $\omega = 6\Delta \approx 1.1$ ). There are discontinuities in the slope of  $\epsilon_2(\omega)$  predicted both here and at  $\omega = 4\Delta$ , where transitions from band to continuum states are first allowed. The abruptness of these effects is characteristic of the model, in that total isotropy implies their onset simultaneously in all directions in  $k$  space. Regardless of this artificiality, however, the magnitude of our results suggests the self-energy effects do play an important role in optical absorption in semiconductors at phonon energies  $\omega$  above the Fermi energy.

#### IV. VERTEX CORRECTIONS

In an effort both to be consistent and to include the most important effects we have investigated the con-

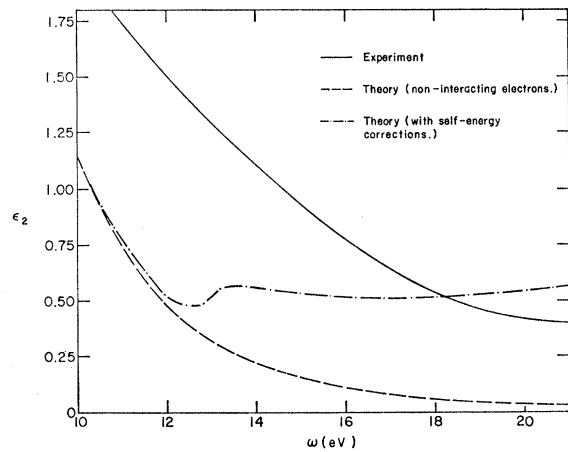


Fig. 7. The imaginary part of the dielectric constant,  $\epsilon_2(\omega)$ , as predicted by theory including self-energy effects [Eqs. (3.10) and (3.13)]. The experimental (solid curve) and infinite lifetime theoretical (dashed curve) results are included for comparison.

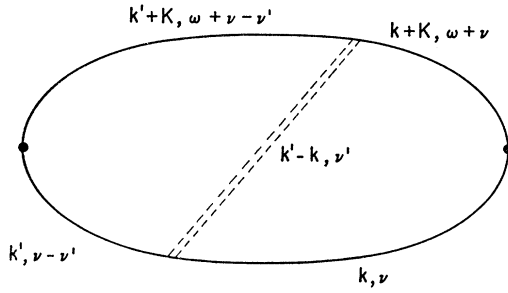


FIG. 8. Vertex correction to the polarizability, accounting in first order for the screened interaction between electron and hole.

tributions of two additional diagrams. The Ward identities,<sup>9</sup> which are generalized statements of the conservation laws, require the inclusion of certain vertex corrections along with each self-energy diagram. The formal statement

$$(\partial/\partial\omega)\Sigma(p \rightarrow 0, \omega) = \Gamma(p \rightarrow 0, \omega), \quad (4.1)$$

where  $\Gamma$  is the vertex function, leads in our case to the diagram of Fig. 8. The intermediate state represents the same physical process as before (an Auger effect). The contribution to the transition probability from this diagram is calculated in Appendix A, and it is found to be an important correction for energies  $\omega$  up to  $\omega \approx 2$ .

There is another type of simple process we have not yet considered, and which one would expect to be important at somewhat lower energies than are the self-energy corrections we have investigated in the previous section. The electron and hole initially created by the incoming photon, in addition to interacting each with the rest of the system, can scatter against one another to give a final state on the energy shell. This can occur for any excitation energy  $\omega > 2\Delta$ , so we are particularly interested in this process below the onset of appreciable self-energy effects (at  $\omega = 6\Delta$ ). We consider, then, the imaginary part of the contribution to the polarizability represented by the diagram of Fig. 9. Before we evaluate this contribution, however, we must point out that our model, as it stands, is inadequate to describe the processes as they occur in a real crystal. The electron is scattered from  $\mathbf{k} + \mathbf{K}$  to  $\mathbf{k}'' + \mathbf{K}$ , where *both*  $\mathbf{K}$ 's are appropriate to  $\mathbf{k}$ :  $\mathbf{K} = -2k_F \hat{\mathbf{k}}$ . The hole, meanwhile, is scattered from  $\mathbf{k}$  to  $\mathbf{k}''$ , and optical recombination can take place only if  $\mathbf{k}'' + \mathbf{K}$  and  $\mathbf{k}''$  correspond to the same reduced zone wave vector. This implies  $\mathbf{k}'' = \mathbf{k}$  in our model, restricting the sum over  $\mathbf{k}''$  to a single term. The contribution thus vanishes as  $1/N$ . However, we realize that our spherical Brillouin zone is an approximation to some polyhedron, where states along any one face (and not too close to an edge) are plane waves mixed primarily with the single reciprocal lattice vector perpendicular to that face. We can build this feature into our

<sup>9</sup> F. Koba, Progr. Theoret. Phys. (Kyoto) 6, 322 (1951) gives the generalized identities. For simplicity, Eq. (4.4) is written for the special case,  $p = 0$ .

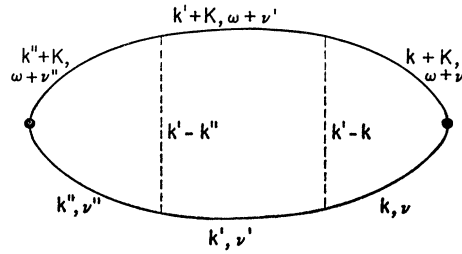


FIG. 9. Vertex correction to the polarizability due to multiple scattering (here, to second order) between the electron and hole.

model simply by neglecting the difference between the  $\mathbf{K}$ 's associated with wave vectors within some reasonable solid angle,  $\delta\Omega$ , of one another. The polarizability will depend only linearly on this solid angle, so it will not be unduly sensitive to the precise choice of a numerical value for  $\delta\Omega$ . The solid angle subtended by a face of the correct Brillouin zone cannot be very different from unity, so we shall use this number in the final numerical evaluation. We shall thus perform the calculation for fixed  $k$  (and  $k'$  therefore within  $\delta\Omega$  of  $k$ ) and then sum over directions  $\hat{\mathbf{k}}$ .

We do the frequency integrals first:

$$\int \frac{d\nu'}{2\pi} G(k'+K, \omega+\nu') G(k', \nu') \\ = i \frac{n(\mathbf{k}') [1 - n(\mathbf{k}'+\mathbf{K})]}{\omega + E_{k'} - E_{k'+K} + i\eta} + i \frac{[1 - n(\mathbf{k}')] n(\mathbf{k}'+\mathbf{K})}{E_{k'+K} - E_{k'} - \omega + i\eta}. \quad (4.2)$$

We are interested in final states in which the pair  $(\mathbf{k}', \mathbf{k}'+\mathbf{K})$  is on the energy shell. [The only other possible final states for this diagram are those for which either  $\mathbf{k}$  and  $\mathbf{k} + \mathbf{K}$  or  $\mathbf{k}''$  and  $\mathbf{k}'' + \mathbf{K}$  are on the energy shell. These are the states considered in Sec. II; the contribution is small because of the coupling factor  $f(k)$ .] Therefore, we want only the real part of Eq. (4.2),

$$\pi |n(k'+K) - n(k')| \delta(\omega - E_k + E_{k'+K}),$$

which ensures that  $\mathbf{k}'$  and  $\mathbf{k}'+\mathbf{K}$  are in different bands and that energy is conserved. We have used the fact that  $n^2(k) = n(k)$  at  $T = 0^\circ$  to simplify this expression. The other frequency integrals are also readily evaluated:

$$- \int \frac{d\nu}{2\pi} \frac{d\nu''}{2\pi} G(k+K, \omega+\nu) G(k, \nu) \\ \times G(k''+K, \omega+\nu'') G(k, \nu'') \\ = - \left[ \frac{n(k)}{\omega + E_k - E_{k+K} + i\eta} + \frac{1 - n(k)}{E_{k+K} - E_k - \omega + i\eta} \right] \\ \times \left[ \frac{n(k'')}{\omega + E_{k''} - E_{k''+K} + i\eta} + \frac{1 - n(k'')}{E_{k''+K} - E_{k''} - \omega + i\eta} \right]. \quad (4.3)$$

Again, we can ignore those contributions for which the pairs at  $\mathbf{k}$  and  $\mathbf{k}''$  are on the energy shell, so we take the principal part of Eq. (4.3). The major contributions occur when the initial and final pairs  $\mathbf{k}$ ,  $\mathbf{k}+\mathbf{K}$  and  $\mathbf{k}'$ ,  $\mathbf{k}'+\mathbf{K}$  are near the Fermi surface (because of the coupling factors  $[f(k)f(k'')]^{1/2}$ ), so we take  $|E_k - E_{k+K}| = |E_{k'} - E_{k'+K}| \approx 2\Delta$ . (This will be accurate as long as  $\omega$  is appreciably larger than  $2\Delta$ .) The result of all frequency integrals is thus approximately

$$-\frac{\pi [2n(k)-1][2n(k'')-1]}{[\omega-2\Delta(2n(k)-1)][\omega-2\Delta(2n(k'')-1)]} \times |n(\mathbf{k}'+\mathbf{K}) - n(\mathbf{k}')| \delta(\omega + E_{k'} - E_{k'+K}). \quad (4.4)$$

We choose  $\mathbf{k}$  to be the polar axis for the  $\mathbf{k}'$  integration. Then the integrand is independent of the azimuthal angle, and the polar angle  $\theta'$  appears only in the factors  $v(\mathbf{k}-\mathbf{k}')$  and  $v(\mathbf{k}-\mathbf{k}'')$ . The  $\delta$  function in Eq. (4.4) is greatly simplified if we recognize that  $\mathbf{k}'$  is rarely at the Fermi surface (once again, as long as we do not consider  $\omega$  too close to  $2\Delta$ ), so we can approximate  $E_k$ , and  $E_{k'+K}$

by free-electron energies. The  $\delta$  function then gives

$$\omega = 4(1 - k' \cos\theta'). \quad (4.5)$$

We have, in addition, the occupation number factor requiring  $\mathbf{k}'$  and  $\mathbf{k}'+\mathbf{K}$  to be in different bands. Since  $\omega > 0$ , this in fact requires  $k' \leq 1$  and  $1 \leq |\mathbf{k}'+\mathbf{K}| \leq 2$ , which by Eq. (4.5) can be written as

$$1 \leq |\mathbf{k}'+\mathbf{K}|^2 = k'^2 + 4(1 - k' \cos\theta') = k'^2 + \omega \leq 4. \quad (4.6)$$

For  $1 \leq \omega \leq 3$  this gives no additional restriction of  $k'$ , but for  $\omega \leq 1$  it puts a lower bound of  $1 - \omega$  on  $|k'|$ . Finally, we note that Eq. (4.5) has a solution for  $|\cos\theta'| \leq 1$  only if  $k' \geq 1 - \omega/4$ .

Before writing down the explicit form for the final momentum integrals, we need expressions for the Coulomb matrix elements.

We approximate the states  $\mathbf{k}'$  by plane waves, but the restriction of  $\mathbf{k}$  and  $\mathbf{k}''$  to the neighborhood of the Fermi surface requires a more careful treatment of these wave functions. Using the notation of Sec. II we find for  $|k| < 1$ ,

$$\frac{4\pi e^2}{[1 + (\alpha_k^+)^2]^{1/2} [1 + (\alpha_k^-)^2]^{1/2}} \sum_{\mathbf{q}} \int d^3r d^3r' (e^{i\mathbf{k}\cdot\mathbf{r}'} + \alpha_k^- e^{i(\mathbf{k}+\mathbf{K})\cdot\mathbf{r}'} - e^{-i\mathbf{k}'\cdot\mathbf{r}'}) \times \frac{e^{i\mathbf{q}\cdot(\mathbf{r}-\mathbf{r}')}}{q^2} (e^{-i\mathbf{k}\cdot\mathbf{r}} + \alpha_k^+ e^{-i(\mathbf{k}+\mathbf{K})\cdot\mathbf{r}}) e^{i(\mathbf{k}'+\mathbf{K})\cdot\mathbf{r}} = \frac{4\pi e^2}{(k-k')^2} \left[ \frac{1}{1 + 1/(\alpha_k^+)^2} \right], \quad (4.7)$$

where we have used the relationship  $\alpha_k^+ \alpha_k^- = -1$  [see Eq. (2.3)]. The angular integral over  $k'$  just involves the denominator  $(\mathbf{k}-\mathbf{k}')^2$  and the  $\delta$  function of Eq. (4.4). We have already discussed the limitations the latter imposes on the range of  $|k'|$ . In addition we write the  $\delta$  function in the form  $(1/4k')\delta[(\omega-4)/4k'+\cos\theta']$  and evaluate  $\cos\theta'$  accordingly in the integrand. From the definition (2.3) we see that  $\alpha_k^+ \geq 1$ , and the factor in brackets in Eq. (4.7) is  $\frac{1}{2}$  at  $k=1$  and increases toward unity as  $k$  is reduced. Although this variation does occur within the range of  $k$  values which contribute appreciably to the integral, we make only a small error by approximating this quantity by a constant; we conservatively take this to be the minimum value,  $\frac{1}{2}$ . We have stated the arguments for the case  $k < 1$ , but it is easily seen that analogous statements can be made for  $k > 1$ .

We can take  $k^2 = 1$  in  $v(\mathbf{k}-\mathbf{k}')$ . The only remaining  $k$  dependence is that of the external vertex factor  $[f(k)]^{1/2}$ , and the calculation reduces to a product of integrals over  $\mathbf{k}$ ,  $\mathbf{k}'$ , and  $\mathbf{k}''$ , with those over  $\mathbf{k}$  and  $\mathbf{k}''$  being identical. From the factor  $[f(k)f(k'')]^{1/2}$  comes the only remaining angular dependence,  $\cos^2\theta$ , if we choose the incoming photon wave vector  $\mathbf{q}$  as the polar axis (recall that  $\mathbf{k}$  and  $\mathbf{k}''$  are parallel to within  $\delta\Omega$ ). The sum over the direction of  $k$  then gives

$$\sum \delta\Omega \cos\theta \int_{\delta\Omega} \cos\theta'' d\Omega \approx 2\pi \delta\Omega \int_{-1}^1 \cos^2\theta d\theta = \frac{4\pi}{3} (\delta\Omega). \quad (4.8)$$

We can then write the total contribution from the diagram, using Eqs. (4.4), (4.7), and (4.8), as

$$\delta\epsilon_2(\omega) \approx \frac{2\delta\Omega}{3(k_F a_0)^3 \pi^3} \left[ \int_0^1 dk \frac{k^2}{\omega - 2\Delta} (f(k))^{1/2} - \int_1^2 dk \frac{k^2}{\omega + 2\Delta} (f(k))^{1/2} \right]^2 \int_{1-\omega/4}^1 dk' \frac{k'}{[1+k'-2(1-\omega/4)]^2}, \quad (4.9)$$

where we have included a factor of 2 from the sum over spin directions, and we have re-expressed  $e^2$  in the dimensionless units of this calculation  $e^2 = (1/k_F a_0)(2\epsilon_F/k_F) \rightarrow 2/k_F a_0$ . The integrals are readily carried out; we find

$$\delta\epsilon_2(\omega) \approx \frac{2\delta\Omega}{3(k_F a_0)^3 \Delta^2 \pi^3} \left\{ \left( \frac{1}{\omega - 2\Delta} \right) \frac{\Delta^2}{4} \left[ 1 + \ln \frac{\Delta^2}{\Delta^2 + 4} + \left( 1 - \frac{\Delta^2}{4} \right) \left( \tan^{-1} \frac{4}{\Delta} \right) \frac{2}{\Delta} \right] - \left( \frac{1}{\omega + 2\Delta} \right) \frac{\Delta^2}{4} \left[ 1 + \ln \frac{\Delta^2 + 4}{\Delta^2} + \left( 1 - \frac{\Delta^2}{4} \right) \left( \tan^{-1} \frac{2}{\Delta} \right) \frac{2}{\Delta} \right] \right\}^2 \{ 8/\omega^2 - 1/\omega \}. \quad (4.10)$$

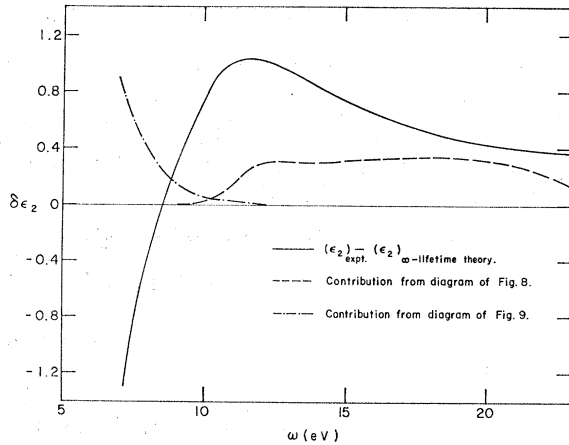


FIG. 10. Vertex corrections to the imaginary part of the dielectric constant. The solid curve is the difference between exponential and infinite lifetime theory values for  $\epsilon_2(\omega)$ . The contribution from the diagram of Fig. 8 is represented by the dashed curve and from that of Fig. 9 by the dot-dashed curve.

Finally, we evaluate this expression for the model semiconductor parameters used above to approximate Ge:  $\Delta=0.18$  and  $k_F a_0=0.92$ :

$$\delta\epsilon_2(\omega) \approx \frac{\delta\Omega}{58.2\pi^3} \left[ \frac{22.3}{\omega+0.36} - \frac{13.2}{\omega-0.36} \right]^2 \times [8/\omega^2 - 1/\omega]. \quad (4.11)$$

This is plotted in Fig. 10 with the solid angle  $\delta\Omega$  chosen as unity. As is clear from the functional dependence of Eq. (4.11) on  $\omega$ , the absorption associated with this effect dies off rapidly at high energies. We recall that in order to make several of the approximations of this calculation we had to restrict  $\omega$  to be appreciably greater than  $2\Delta$ . It is therefore unreasonable to place any confidence in our results below  $\omega < 0.6$  or so, but the numbers, which have been conservatively estimated, certainly suggest that electron-hole scattering may be of some importance in the absorption of photons of energy  $\omega \leq 1$ . However, for larger  $\omega$  the contribution of Appendix A dominates.

## V. CONCLUSIONS

The suggestion<sup>3</sup> that electron-electron interactions significantly modify the high-frequency optical absorption of semiconductors has been verified. Although the experimental results for the dielectric constant at these frequencies show no dependence on band-structure details, the isotropically extended nearly-free-electron model which we have used for explicit calculations is sufficiently unrealistic that precise agreement with experiment could not be expected (and has not, indeed, been found). We have already pointed out, in particular, the sudden onset of each effect, created by the exact isotropy of the model and the resultant singularity in the density of states. This spherical band structure is

not realizable for any crystal potential. In fact, we have shown that in order to obtain sensible results for vertex corrections it is necessary to flatten slightly the spherical zone boundary, with its associated continuously varying reciprocal lattice vectors, into a more realistic polyhedron. The model we have used in which only two plane waves are mixed in forming band states overestimates the rate of decrease of oscillator strengths away from the zone boundaries, as can be seen explicitly from more accurate band structure calculations. However, let us reiterate that the excessively steep dropoff of  $\epsilon_2(\omega)$  for large  $\omega$  is a general result for even the most accurate of band-structure calculations since it follows from the general  $f$ -sum rule.<sup>3</sup> In spite of these inadequacies of the model we believe that the Auger processes and electron-hole scatterings we have described are reasonable representations of effects that occur in real crystals. Thus, the magnitude and general behavior of the contribution to  $\epsilon_2(\omega)$  which we have calculated are representative of those from corresponding sources in real semiconductors—with the structure we have found to be smoothed out by crystalline anisotropy and by the more complex nature and mixing of the actual band states.

We have used an admittedly deficient model, but one which contains the essential feature of allowed interband optical transitions while remaining sufficiently simple to treat thoroughly in lowest approximation (noninteracting electrons). We do not claim to have given an exhaustive analysis of the corresponding diagrammatic perturbation theory, but rather to have examined a consistent set of graphs representing clearly important physical processes. Very general arguments have been used<sup>3</sup> to demonstrate the inadequacy of a free-(Bloch)-electron picture; we have indicated that consideration of the many-body effects of the Coulomb interaction between electrons substantially reduces the discrepancy between theory and experiment.

## ACKNOWLEDGMENTS

The authors thank Professor David Pines for suggesting the investigation of this problem. They also thank Professor Richard A. Ferrell, Professor Richard E. Prange, and Professor J. Robert Schrieffer for numerous discussions, and Professor Henry Ehrenreich for detailed numerical data on germanium experiments.

Finally, we wish to express our appreciation to the Laboratoire de Physique of the Ecole Normale Supérieure, Paris, France, where this work was begun while one of us (A.B.) was a National Science Foundation postdoctoral fellow and the other (D.H.) a U. S. Air Force Office of Scientific Research postdoctoral fellow.

## APPENDIX A: EVALUATION OF THE DIAGRAM OF FIG. 8

For exactly the same reason as we discussed in Sec. IV, with reference to the diagram of Fig. 9, the present contribution vanishes within the pure spherical band

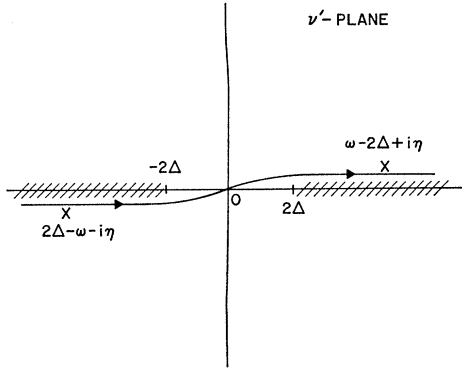


FIG. 11. Contour for the  $\nu'$  integration of the Appendix. The only poles crossed when the contour is shifted to the imaginary axis are the two indicated at  $\nu' = \pm(\omega - 2\Delta + i\eta)$ .

model. In this case it is the intermediate photon momentum  $\mathbf{k} - \mathbf{k}'$  which can only be zero if the electron at  $\mathbf{k}' + \mathbf{K}$  is to recombine with the hole at  $\mathbf{k}'$  and emit an optical photon (wave vector  $\approx 0$ ). We therefore modify the model just as we did in that section, ignoring differences in reciprocal lattice vector for momenta within a solid angle  $\delta\Omega$ . The dominant momentum transfers  $\mathbf{k} - \mathbf{k}'$  will still be small, so the appropriate screening is given by  $\epsilon(q \rightarrow 0, \nu')$ , which we have calculated within the RPA in Sec. II.

The integrals simplify considerably if we take into account, as in Sec. IV, the rapid variation of the vertex factor  $[f(k)f(k')]^{1/2}$ . Only the regions  $k, k' \approx 1$  contribute appreciably, and we can take  $\epsilon_k \approx \Delta[1 - 2n(k)]$ ,  $\epsilon_{k'} \approx \Delta[1 - 2n(k')]$ . We then have for the  $\nu$  integration:

$$\begin{aligned} & \int \frac{d\nu'}{2\pi} \{ [\omega + \nu - \nu' - E_{k'+K}(1 - i\eta)] [\nu - \nu' - E_{k'}(1 - i\eta)] [\omega + \nu - E_{k+K}(1 - i\eta)] [\nu - E_k(1 - i\eta)] \}^{-1} \\ & \approx in(k') \left\{ \frac{n(k)}{\omega - 2\Delta} \left( \frac{1}{\nu'} \right) \left[ \frac{1}{\omega + \nu' - 2\Delta + i\eta} - \frac{1}{\omega - \nu' - 2\Delta + i\eta} \right] \right. \\ & \quad \left. + \frac{1 - n(k)}{\omega + \nu'} \left[ \left( \frac{1}{\omega - 2\Delta} \right) \left( \frac{1}{\nu' - 2\Delta + i\eta} \right) - \left( \frac{1}{\omega + 2\Delta} \right) \left( \frac{1}{\nu' + 2\Delta - i\eta} \right) \right] \right\} \\ & \quad + i[1 - n(k')] \left\{ \frac{n(k)}{\nu' - \omega} \left[ \frac{1}{\omega - 2\Delta} \left( \frac{1}{\nu' + 2\Delta - i\eta} \right) - \frac{1}{\omega + 2\Delta} \left( \frac{1}{\nu' - 2\Delta + i\eta} \right) \right] \right. \\ & \quad \left. + \frac{1 - n(k)}{\omega + 2\Delta} \left( \frac{1}{\nu'} \right) \left[ \frac{1}{\omega - \nu' + 2\Delta - i\eta} - \frac{1}{\omega + \nu' + 2\Delta - i\eta} \right] \right\}. \quad (\text{A1}) \end{aligned}$$

The remaining frequency integral, over  $\nu'$ , is to be computed along a contour determined by the singularities of  $1/\epsilon(\nu')$ . The situation differs from that of the free-electron case, in that interband transitions make possible excitations for all energies  $\nu' \geq 2\Delta$ , and the branch points in  $1/\epsilon(\nu')$  are at  $\pm 2\Delta$ , as indicated in Fig. 11. We follow Quinn and Ferrell in moving the contour to the imaginary axis:  $\nu' = iV$ , with  $V$  real. We use the property  $\epsilon(k, \omega) = \epsilon(k, -\omega)$  to rewrite the integral

$$i \int_{-\infty}^{\infty} dV \frac{F(iV)}{\epsilon(0, iV)} = \frac{i}{2} \int_{-\infty}^{\infty} dV \frac{F(iV) + F(-iV)}{\epsilon(0, iV)}. \quad (\text{A2})$$

We now invoke the relation  $\epsilon(0, iV) = \epsilon^*(0, -iV)$  to argue that this is pure imaginary. The only real part of the polarizability comes from the poles of Eq. (A1) crossed when the contour is shifted to the imaginary axis. This contribution comes from the first term only in Eq. (A1); we find for the contribution to  $\epsilon_2(\omega)$

$$\delta\epsilon_2(\omega) = 2(4\pi e^2)^2 \int \frac{d^3k}{(2\pi)^3} \int_{\delta\Omega} \frac{d^3k'}{(2\pi)^3} [f(k)f(k')]^{1/2} \left[ n(k)n(k') \left( \frac{1}{\omega - 2\Delta} \right)^2 (k - k')^{-2} \right] \text{Im} \frac{1}{\epsilon(0, \omega - 2\Delta)}. \quad (\text{A3})$$

As in Sec. IV the only dependence on the direction of  $\mathbf{k}$  comes from the  $\cos^2\theta$  in the vertex factor  $[f(k)f(k')]^{1/2}$ . We take  $\mathbf{k}$  to be the polar axis for the  $\mathbf{k}'$  integration, and we find

$$\int_{\delta\Omega} d\Omega_{k'} (k - k')^{-2} = 2\pi \int_{1 - \delta\Omega/2\pi}^1 d \cos\theta' (k^2 + k'^2 - 2kk' \cos\theta')^{-1} = \frac{\pi}{kk'} \log \left[ \frac{(k - k')^2 + 2kk' \delta\Omega/2\pi}{(k - k')^2} \right]. \quad (\text{A4})$$

The integral over  $k'$  contains the factor  $[f(k')]^{1/2}$ , which decreases rapidly from its value at  $k'=1$ , effectively restricting  $k'$  to a small region near unity. We therefore can put an upper bound on the integral by replacing

$f(k')$  by  $f(1)$  for  $1-\alpha \leq k' \leq 1$  and by zero for smaller  $k'$ , with  $\alpha \ll 1$ . We can then perform the  $k'$  integration trivially:

$$\int_{1-\alpha}^1 dk' k' \ln \left[ \frac{(k-k')^2 + 2kk'\delta\Omega/2\pi}{(k-k')^2} \right] \\ = \frac{1}{2} [1 + k^2(1-2\gamma^2)] \ln(1-2k\gamma+k^2) - \frac{1}{2} [(1-\alpha)^2 + k^2(1-2\gamma^2)] \ln[(1-\alpha)^2 - 2k\gamma(1-\alpha) + k^2] - (1-k^2) \ln(1-k) \\ - [k^2 - (1-\alpha)^2] \ln(k-1+\alpha) + k\alpha(1-\gamma) + 2\gamma k(1-\gamma^2)^{1/2} \left[ \tan^{-1} \frac{1-\gamma k}{k(1-\gamma^2)^{1/2}} - \tan^{-1} \frac{1-\gamma k-\alpha}{k(1-\gamma^2)^{1/2}} \right], \quad (\text{A5})$$

where we have set

$$1 - \delta\Omega/2\pi \equiv \gamma \approx 0.84 \quad (\text{for } \delta\Omega = 1). \quad (\text{A6})$$

This must now be integrated over  $k$ . Again there is a vertex factor  $[f(k)]^{1/2}$ , which we replace by its value at  $k=1$  in the range  $1-\alpha < k < 1$ . The difference between the two  $\tan^{-1}$  terms is small, so we simplify the integrand by expanding

$$k(1-\gamma^2)^{1/2} \left[ \tan^{-1} \frac{1-\gamma k}{k(1-\gamma^2)^{1/2}} - \tan^{-1} \frac{1-\gamma k-\alpha}{k(1-\gamma^2)^{1/2}} \right] = \alpha + O(\alpha^2). \quad (\text{A7})$$

In the same spirit we make approximations of two of the logarithms, keeping in mind that  $k$  is restricted to the interval  $1-\alpha \leq k \leq 1$ :

$$\ln(1-2k\gamma+k^2) = \ln 2(1-\gamma) + O(\alpha), \\ \ln[(1-\alpha)^2 - 2k\gamma(1-\alpha) + k^2] = \ln 2(1-\gamma) + O(\alpha). \quad (\text{A8})$$

The final integral over  $k$  is now straightforward. We find

$$\int_{1-\alpha}^1 dk k [\text{Eq. (A5)}] = \alpha^2 \ln 2(1-\gamma) - 2\alpha^2(1-\alpha) \ln \alpha + (2+\gamma)\alpha^2 + O(\alpha^3). \quad (\text{A9})$$

We can now return to the expression (A3) for the contribution to the dielectric constant:

$$\delta\epsilon_2(\omega) \approx \frac{f}{3\pi^2 k_F a_0} \frac{1}{\Delta^2(\omega-2\Delta)^2} \text{Im} \frac{1}{\epsilon(0, \omega-2\Delta)} \times \text{Eq. (A9)}. \quad (\text{A10})$$

The dependence of this on  $\omega$  arises entirely from the factor

$$(1/2)(\omega-2\Delta)^{-2} \text{Im} 1/\epsilon(0, \omega-2\Delta). \quad (\text{A11})$$

The behavior of this function can be found either from the experimental curves for  $\text{Im}(1/\epsilon)$  or from our own RPA infinite lifetime calculation of Sec. II. In Fig. 10 we have indicated the onset at  $\omega=4\Delta$  (the smallest energy possible for creation of two electron-hole pairs) and we have joined smoothly to the experimental values for Eq. (A11). We see a rise to a roughly constant value  $\approx 0.3$  until the energy corresponding to the peak of  $\text{Im} 1/\epsilon$  (at  $\omega-2\Delta \approx 1.3$ ) is reached and then a rapid falloff due to both factors in the product (A11). The ratio of this function to  $\delta\epsilon_2(\omega)$  depends on the precise choice of the cutoff parameter  $\alpha$ . For the reasonable value  $\alpha=0.1$  we find this ratio to be approximately unity. We must recognize, however, that the approximations made for  $f(k)$  may have introduced errors of a factor of 2 or so in these results.